Electrical measurements in μ-EDM

Carlo Ferri[1], Atanas Ivanov[2] and Antoine Petrelli[3]

[1] Via XI Febbraio 40, 24060 Castelli Calepio, BG, Italy.*

[2] Cardiff University, Cardiff CF24 3AA, UK.*

[3] ISAT, Université de Bourgogne, 58027 Nevers, France.*

E-mail: ferric@cardiff.ac.uk, ivanov@cardiff.ac.uk

Abstract. The phenomena occurring between the electrodes in electric discharge machining when manufacturing features on the micro-metre scale (μ-EDM) is not fully understood. Poor quantitative knowledge of the sources of variability affecting this process hinders the identification of its natural tolerance limits. Moreover, improvements in measuring systems contribute to the acquisition of new information that often conflicts with existent theoretical models of this process. The prime objective of this paper is to advance the experimental knowledge of μ-EDM, by providing a measurement framework for the electrical discharges. The effects of the electrodes metallic materials (Ag, Ni, Ti, W) on the electrical measurements defined in the proposed framework are analysed. Linear mixed-effects models are fitted to the experimental data using the Restricted Maximum Likelihood Method (REML). The main conclusion drawn is that the discharge current and voltage as defined and measured in this framework do significantly depend on the electrodes material even when keeping all the other machining conditions unchanged.

Submitted to: *J. Micromech. Microeng.*

Keywords: μ-EDM, micro-EDM, micro electric discharge machining, linear mixed-effects models.

* This investigation was carried out while the authors were at the Manufacturing Engineering Centre of Cardiff University.

1. Introduction

Electrical discharge machining (EDM) is the process of removing material from two electrodes, the workpiece and the tool. When these electrodes are submerged in a liquid dielectric bath, the pulses of voltage that are applied to them cause a sequence of breakdowns and recoveries of the in-between dielectric. A pulsed flow of current therefore takes place between the electrodes. Each of these pulses is also referred to as a current discharge or, simply, a discharge.

When the electrical parameters driving the process are set to their minimum values, minimum electric instant power and minimum energy are expected to be released into both dielectric and electrodes. In this way, features of micrometric size are produced on the workpiece electrode. The designation 'micro electric discharge machining' (μ-EDM) is therefore used in these cases.

The smaller the nominal energy per pulse of current becomes, the smaller the expected value of the unit removal (UR) is. Unit removal is defined as 'the part of a workpiece removed during one cycle of removal action' [1]. In μ-EDM, UR is therefore the material removed from the workpiece electrode during one discharge.

The technological progress in electrical and electronic components together with the constant research effort in the design and manufacture of purpose-built μ-EDM generators strive to minimise the nominal energy per pulse of current. Maximum nominal discharge energies per pulse as small as approximately $3\,n$J obtained using an RC discharge circuit have been reported by Egashira *et al* [2].

A large number of uncontrollable or not-yet-convenient-to-control factors are expected to affect significantly the instant values of the voltage and of the current intensity flowing between the two electrodes. This holds regardless of the set-up parameters for the power generator (i.e. the nominal values of voltages, current, energy, etc.) and for the positioning system of the electrodes.

Typical set-up parameters of a transistor-based power generator are the open circuit voltage, V_0, the mean current, I, the duration of the pulses of voltage, t_i, the time interval between successive pulses of voltage, t_0. Figure 1, which has been derived on the basis of a machine manual [3], illustrates these parameters together with some quantities defined and measured in this investigation. The first are displayed as boxed characters in figure 1, the second as plain characters.

[Figure 1 about here.]

Significant advantages of a transistor type isopulse generator over RC pulse generators in μ-EDM semifinishing and finishing operations have been discussed by Han *et al* [4].

Typical uncontrolled factors are the actual local distance between the electrodes where a discharge takes place (spark gap), the actual strength of the dielectric in the spark gap, the degree of contamination of the spark gap, the motion characteristics of the liquid dielectric between the electrodes, the local composition and physicochemical local properties of the electrodes materials and of the dielectric medium.

The set-up parameters of figure 1 identify ideal relationships between the voltage, the current and the time. Therefore the instant electrical power as a function of the time and the electrical energy of a pulse can be calculated from them.

However, it is argued that this power function and this energy are just nominal. In fact the uncontrolled factors mentioned above cause the actual dependence of voltage and current on the time to differ significantly and unpredictably from their nominal representation of figure 1.

As a consequence, the UR is expected to be affected by a source of variability corresponding to the dispersion of the electrical characteristics of the discharges. In this context, the terms electrical characteristics of a discharge refer to current and voltage dependence on the time during a discharge. For a particular pair of electrodes, this variability of the UR is then the primary cause of the natural tolerance of the process.

It is envisaged that two directions of investigation can significantly contribute to quantify and possibly to reduce the natural tolerance of the EDM process.

The first is an extended effort in limiting the variability of the discharge electrical characteristics by analysing the effect that the aforementioned uncontrolled factors exert on them and, consequently, by extending the control on them.

The second consists in the quantitative identification of the relationship between the UR and the electrical characteristics of a discharge.

On one hand, Dauw [5] undertook research activities in both of these directions by developing a classification of the discharge electrical characteristics and an adaptive control system based on this classification. On the other hand, Weck [6] focused his research on the second direction while presenting an adaptive control founded on the identification of the relationship between some discharge electrical characteristics and the removal process. The material removal contribution of discharges previously subdivided into groups is the main purpose of the investigation performed by Cogun [7].

Evidence of similar studies in the μ-EDM field has not been found. Investigations of the effect of electrodes' materials on the discharge electrical characteristics during μ-EDM operations have also not been found. Such investigations can contribute to shed light upon the nature of the differences between wear ratios of different electrode materials reported in Ivanov *et al* [8]. They can in fact determine whether these differences in wear ratios are also contributed to by the influence of the materials properties on the discharge electrical characteristics (voltage, current and derived quantities).

Electric breakdown in liquid dielectric is a major area of interest in the studies of electrical insulation in alternating current (AC) and direct current (DC) power generation and transmission [9]. Dielectric oil is typically used in transformers to provide both high voltage insulation and cooling. The focus of these studies is on modelling the electrical insulation and the breakdown phenomena of the dielectric medium [9, 10]. Whereas in EDM studies, the erosion mechanism on the electrodes is at the centre of the research efforts [11, 12, 13, 14].

In addition, the experimental conditions in these two research areas present

significant differences. In EDM, the relative position and the shapes of the electrodes are changing during the process. They are continuously repositioned by closed-loop controlled actuators, while their form is also evolving.

Central to EDM is the removal of material from the workpiece-electrode caused by series of discharges. Each of these discharges and the whole sequence of them should therefore be investigated. Central to electrical insulation is the occurrence of the first breakdown, which has to be prevented, between two electrodes at a constant distance and with carefully designed constant form.

The composition of the dielectric between the electrodes is expected to evolve significantly more in EDM than in experimental settings typical of electrical insulation studies [9]. In this last area of research [9] and even more so in EDM investigations, the nature of the studies is often empirical with most measurements taken at electrical terminals of voltage and current. No direct information on the electrical field distribution throughout the volume between the electrodes is accessible.

Extending to μ-EDM the empirical results obtained in the neighbouring area of electrical insulation may therefore appear questionable owing to the typically different experimental conditions of the two domains.

In this paper, which extends the exploratory analysis presented in Ferri *et al* [15], an experimental framework is proposed in order to measure electrical quantities at electrical terminals during machining operations. The framework is twofold. First, the definitions of generic waveform and average waveform are introduced. Subsequently, operational definitions of electrical properties of the average waveform are provided. The effects of four different electrode materials (Ag, Ni,Ti, W) on both mean and variability of these electrical properties are then estimated by fitting linear mixed-effects (LME) models to the data using the restricted (or residual) maximum likelihood method (REML) [16].

2. Experimental Set-up

A commercially available EDM machine was deployed in this investigation. The EDM machine was set up to deliver the minimum nominal energy during each discharge. According to Masuzawa [1], this condition is sufficient and necessary to place a manufacturing operation in the micro manufacturing domain. The set-up of the transistor-based generator used is summarised in table 1.

[Table 1 about here.]

The values displayed in table 1 are of the same order as those that can be set on a specific brand of EDM machine marketed by its worldwide-known manufacturer as μ-EDM machine during the first half-decade of the twenty first century. Moreover, Han *et al* [4] reported for their purpose-built experimental transistor type isopulse generator $V_0 = 80\,V$, $t_0 = 400\,ns$, $i_{max} = 1.2$ and $0.6\,A$, $t_e = 80$ and $30\,ns$ for semifinishing and finishing operations, respectively.

The comparison between the investigations of Egashira *et al* [2] and of Han *et al* [4] places this study in the border region between the micro- and meso-scale of

the EDM applications. Notwithstanding, the main objective of this investigation is to define a consistent measurement framework whose nature is insensitive to the nominal set-up parameters of the process and/or the dimensional scale of the manufactured parts (macro-, meso-, micro-scale).

Current and voltage measurements were taken by means of a current transformer (current probe) and a passive voltage probe (10 MΩ, 14 pF, with attenuation factor $10x$ and bandwidth 200 MHz at -3 dB), respectively. The technical specifications of the current probe are displayed in table 2.

[Table 2 about here.]

Both probes were connected to an oscilloscope whose specifications are shown in table 3.

[Table 3 about here.]

The dielectric used was a commercially available, purpose designed liquid hydrocarbon whose main physicochemical properties are presented in table 4.

[Table 4 about here.]

The overall test rig is illustrated in figure 2.

[Figure 2 about here.]

To measure the voltage, the oscilloscope was set up with a vertical scale of two volts per division, i.e. 2 V/div, corresponding to an actual value of 20 V/div due to the $10x$ voltage probe used.

To measure the current, a vertical scale of 500 mV/div was set up, corresponding to an actual value of 500 mA/div owing to the ratio V/A=1 of the used current probe.

The time scale was set at 200 ns/div. An overall time interval of 2 μs was therefore monitored.

When connecting the two probes to the oscilloscope, a DC coupling option was selected to enable constant components of the probed voltage and current to be measured.

The recording action of the oscilloscope starts when a particular event, called the trigger event, is detected. In this investigation, the oscilloscope was set up so that a trigger event occurs when the current exceeds the pre-specified level of 310 mA.

The documentation supplied by the machine manufacturer defines time-on (T_{ON}) as discharge time and time-off (T_{OFF}) as the 'period between two consecutive discharges'.

However, an experimental investigation suggested that time-on is solely connected with the train of pulses of voltage regardless of any current flowing through the electrodes. In this train of voltage pulses, the time duration of each pulse having an average value of about V_0 seems to coincide with T_{ON}. On the other hand, the time interval between two consecutive pulses of voltage appears to coincide with T_{OFF}. In figure 3, which supports these interpretations, the set-up parameters of the power generator are chosen so as this evidence is made clearer (V_0 = 80 V, T_{ON} = 40 μs, T_{OFF} = 130 μs, I = 0.5 A, V_{SERVO} = 50 V).

[Figure 3 about here.]

In this figure, only two current pulses are visible on the second channel (the two vertical segments at the right bottom side), whereas the train of pulses of voltage on the first channel (top) still maintains the T_{ON} - T_{OFF} pattern. Therefore, the parameters T_{ON} and T_{OFF} do not appear directly connected with the occurrence of a current flow through the electrodes.

It is then argued that the parameters T_{ON} and T_{OFF} are different from the parameters t_0 and t_i in figure 1, in spite of the their definitions in the machine documentation. This finding is an invitation to the researchers in the EDM and μ-EDM areas to measure directly the effects that set-up parameters of a piece of complex equipment such as an EDM power generator actually have on the process.

3. Definitions

Each measurement performed using the oscilloscope gave a time series of 1000 voltage values where the sampling interval was constant. This time series was acquired on the occurrence of the trigger event defined in the previous section. In this context, the time series of 1000 current intensity values is defined as a *current generic waveform*. Correspondingly, the concurrent time series of 1000 voltage values is defined as a *voltage generic waveform*. As motivated in section 1, these generic waveforms differ significantly and unpredictably from the nominal pulse shapes of voltage and current, i.e. $v_{\mathrm{N}}(t)$ and $i_{\mathrm{N}}(t)$, illustrated in figure 1.

When the set-up option called 'average acquisition mode' is activated on the oscilloscope, a pre-specified number of current and voltage generic discharges are detected and their values are averaged into two average time series, which are displayed on the screen of the oscilloscope. In this investigation, the displayed current (voltage) time series is the average of 256 current (voltage) generic waveforms. Hereafter, the current and voltage time series resulting from the averaging process are referred to as *current average waveform* and *voltage average waveform*, respectively. Their product is then defined as the *instant power average waveform*. For convenience, this product is performed directly by the oscilloscope.

For each of the four electrode metals considered in this study (Ag, Ni, Ti and W), Figure 4 shows one instance of the voltage, current and instant power average waveforms, indicated with *v(t)*, *i(t)* and *p(t)*, respectively. All the units of measurements used in figure 4 have been described in section 2, with the exception of the instant power *p(t)*, which has units 10 W/div and 200 ns/div on the ordinate and the abscissa respectively. These units have been derived on the basis of the definition of instant power and on the basis of the set-up for the other measured quantities.

[Figure 4 about here.]

These average waveforms are then used to define physical quantities of interest, which in turn are measured directly on the oscilloscope using built-in functionalities.

Among them, those for taking gated measurements were especially useful. Nine electrical quantities have been defined:

- $\bar{v}_0$, the average of the voltage average waveform measured from 200 ns before the occurrence of the trigger event to the instant when the current begins to flow, i.e. to the abscissa of first positive point on the current average waveform. Let this point be named A. Henceforth, $\bar{v}_0$ is also called 'measured open circuit voltage'.
- $\bar{v}_e$, the average of the voltage average waveform during the current flow measured from the abscissa of A to the instant after the last positive value on the current average waveform. Let this point be named B. Hereafter, $\bar{v}_e$ is also referred to as 'discharge voltage'.
- t_e, the time duration of current flow measured on the current average waveform. It is computed as the time interval between the points A and B. Below t_e is also referred to as 'discharge duration'.
- $\bar{i}$, the average intensity of the current flow measured on the average current waveform during the discharge duration t_e. Alternatively, the average of the current average waveform during t_e. Henceforth, for brevity, $\bar{i}$ is also called 'discharge current'.
- i_{max}, the maximum value of current average waveform during t_e.
- t_{max}, the time interval between the instant when the current begins to flow and the instant when the current is at its maximum. It is the difference between the abscissae of i_{max} and A.
- $\bar{P}$, the average of the instant power average waveform during t_e. For brevity, $\bar{P}$ is also referred to as 'discharge power'.
- P_{max}, the maximum of the instant power average waveform during t_e.
- e, the discharge energy of the instant power average waveform, namely, the integral of the instant power average waveform during t_e. By this definition, it is also equal to the product $\bar{P} \cdot t_e$.Henceforth, the quantity e is also referred to as 'discharge energy'.

In figure 4, values of t_e are also shown for each of the four examples illustrated.

When the objective is to characterise the general tendency of the machining process, it appears appropriate to compare nominal pulses (figure 1) with the corresponding average waveforms (figure 4) rather than with the corresponding generic waveforms. In fact the generic waveforms, owing to the large variability of the local inter-electrodes conditions (cf. section 1) have a vast range of different shapes all significantly differing between themselves and from the nominal pulses (cf. Dauw [5]). Instead the average waveforms are, on one hand, less variable by definition (the variance of an average of independent identical variables is $1/n$ the variance of the single original variable). On the other hand, they and their variability are more representative of the whole machining process. The averaging process in fact attenuates the effect on the electrical measurements of accidental and less frequent phenomena between the

electrodes. Moreover, considering average waveforms reduces by several orders the otherwise technically unsustainable experimental effort and data collection burden.

A comparison of nominal pulses with average waveforms is quantitatively performed by contrasting nominal set-up parameters of the generator (figure 1) with actual values of the electrical quantities defined above and founded on average discharges waveforms (figure 4). In figure 1, a match between widespread set-up parameters of transistor-based generators (boxed symbols) and some measurements defined above (non-boxed symbols) is also suggested.

4. Design of the experiment

The experimental activities have been designed in order to block the effects of potential sources of variability of the μ-EDM process not explicitly targeted.

This is one reason why metals with purity higher than 99.9 % were selected for the electrodes in the tests. It is in fact anticipated that potentially inflated variability conditions in μ-EDM operations can arise due to locally heterogeneous physicochemical properties of the electrodes such as, for instance, thermal conductivity, electrical conductivity and ionisation energy. If metals with high degree of purity are used as electrodes, it should therefore be easier to detect effects of electrode materials on electrical properties of average waveforms.

To some extent this approach appears consistent with the observations of Han *et al* [17] regarding the effects of material microstructural inter-grain defects on the performances of μ-EDM.

Silver (Ag), Nickel (Ni), Titanium (Ti) and Tungsten (W) were selected as electrode materials so that a broad range of physicochemical properties appearing in the periodic table of the elements was covered.

It is then expected that these electrical properties can be significantly different when the same anodic material is used with different cathodic materials. This expectation appears consistent with the fact that, in their manuals, the manufacturers of EDM equipment usually suggest different set-up parameters of the generator for machining different workpiece materials (e.g. steel, aluminium), even though the electrode material remains the same (copper, for instance). Thus, although it may appear an unusual decision to the practitioners in the field, in each test the electrode material for the anode was the same as for the cathode. In this way, the results of the study are an exclusive property of a specific metal, regardless of the expected anode-cathode interaction effect on the average waveforms.

For each individual material, the initial shape of the electrodes, especially of their tips, is qualitatively the same in each test carried out. It is anticipated, in fact, that the initial shape of the electrodes may constitute a further source of variability affecting the electrical properties of average waveforms. All the electrodes were in the shape of rods with circular cross section of diameter one millimetre.

On one hand, this size of the electrode is admittedly unusual for μ-EDM operations,

where commercially available W and WC rods and pipes may have diameters as small as 80 and 120 μm, respectively. On the other hand, it offers the advantage that a broader range of pure metals is readily available in almost identical shape and size, without the need of pre-machining the electrodes (for instance using electric discharge grinding). This last process may alter the physicochemical properties of the selected materials introducing an avoidable nuisance on the experiment. The measurement framework presented in this study does not appear to be affected by the particular size and shape of the electrodes.

In order to limit the set-ups of the machine to an affordable number, the experiment was carried out in a sequence of five experimental units, hereafter also referred to as blocks. A block is characterised by the fact that, within it, tests pertaining to the same electrode material were performed in succession, rather than being randomly assigned to the sequence order. In each experimental unit, five average waveforms of current, voltage and instant power were recorded for each of the four electrodes materials. On these average waveforms, measurements of the nine electrical quantities defined in the previous section were taken. For each of the four materials, 25 measurements of each of the nine electrical properties were therefore taken. The overall experimental effort amounted to 900 measurements.

5. Results

The nine electrical quantities defined in section 3 have been analysed according to the methods presented in Pinheiro and Bates [16]. These methods also document the library `nlme` used in this study within the free software environment and language for statistical computing `R` [18]. The data pertaining to these quantities were fitted with linear mixed-effects models of the following generic form:

$$\mathbf{y}_i = \mathbf{X}_i\boldsymbol{\beta} + \mathbf{Z}_i\mathbf{b} + \mathbf{e}_i \qquad i = 1, \ldots, 5 \tag{1}$$

where, adopting a widespread convention, Greek characters are used to represent unknown parameters, whereas Latin characters are used to indicate both random variables and their known or unobservable realizations.

$\mathbf{y}_i = [y_{i1}\ y_{i2}\ \ldots\ y_{i20}]^t$ is the response vector of all the realisations in the *i-th* block for the electric quantity under investigation (for instance v_e or $\bar{i}$).

$\boldsymbol{\beta} = [\beta_0\ \beta_1\ \beta_2\ \beta_3]^t$ is the vector of the fixed effects associated with the electrode materials. Each material of the electrodes is set as an experimental fixed-effects factor, β_j with $j = 0, 1, 2, 3$. In fact, one of the objectives of this experiment is to determine whether there are systematic differences in the response variable to arise from the different electrodes materials investigated.

In the more general form of the model, $\mathbf{b} = [b_0\ b_1\ b_2\ b_3]^t$ is the column vector of random variables representing the random effects exerted by the experimental unit on the response $\mathbf{y}_i$ of the electrode material identified by the b_j's subscripts with $j = 0, 1, 2, 3$ (for instance Ti=0, W=1, Ag=2, Ni=3). In principle in fact such random

effects may be different for each of the electrode materials considered and may also be correlated.

An experimental unit represents a known source of potential variability in the experiment. Given an electrode material, the 25 realisations of the response variable are grouped in sets of five observations, each set corresponding to one block. If a lurking nuisance occurs while performing the five consecutive tests in a block for that electrode material, for instance a temporary series of surges in the circuits of the generator, then the variability of the whole series of 25 measurements across the five blocks increases. Moreover, if this lurking nuisance occurs in a block while testing two different electrodes materials, the corresponding random effects may result correlated. These possibilities are accounted for by considering the column random vector $\mathbf{b}$ as normal distributed with zero mean and variance-covariance matrix with the sole constraints of being a positive-definite, symmetric 4×4 matrix $\mathbf{\Psi}$, namely $\mathbf{b} \sim \mathcal{N}(\mathbf{0}, \mathbf{\Psi})$ (model A).

It is however anticipated that models with more stringent constraints on $\mathbf{\Psi}$ can constitute viable alternative to model A. Therefore four additional models are considered in this study:

- model B, with independent random effects, i.e. $\mathbf{\Psi} = diagonal\,[\sigma_0^2\ \sigma_1^2\ \sigma_2^2\ \sigma_3^2]$;
- model C, with random effects independent and same variances in the random interaction effects, i.e. $\mathbf{b} = [b_{main}\ b_{int,0}\ b_{int,1}\ b_{int,2}\ b_{int,3}]^t$ and $\mathbf{\Psi} = diagonal\,[\sigma_{main}^2\ \sigma_{int}^2\ \sigma_{int}^2\ \sigma_{int}^2\ \sigma_{int}^2]$;
- model D, with a sole random effect for the blocks and no interaction random effect between the blocks and the electrodes materials. This implies that $\mathbf{b}$ is reduced to the scalar $b_i \sim \mathcal{N}(0,\ \sigma_b^2)$;
- model E, without any random effect, namely $\mathbf{Z}_i = \mathbf{0}$.

The column vector $\mathbf{e}_i = [e_{i1}\ e_{i2}\ \ldots\ e_{i20}]^t$ represents unobservable realizations of random variables which account for all those sources of variability that are not explicitly considered in the model. They are called errors. Their spread, by definition, expresses the perceived variability of the manufacturing process in terms of the observed electrical quantity (the $\mathbf{y}_i$'s). The $\mathbf{e}_i$'s are considered as the end results of the occurrence of several independent causes, each of which is contributing to the $\mathbf{e}_i$'s with a small random amount. Under these circumstances, and in virtue of the central limit theorem, it appears reasonable to assume $\mathbf{e}_i \sim \mathcal{N}(\mathbf{0}, \sigma^2\mathbf{I}_{20})$, where $\mathbf{I}_{20}$ is the 20×20 identity matrix.

The matrix $\mathbf{X}_i$ has dimensions 25×4 in all the models. The matrix $\mathbf{Z}_i$ has dimensions 25×4 in models A and B, whereas in models C and D it has dimensions 25×5 and 25×1, respectively. In model E it holds $\mathbf{Z}_i = \mathbf{0}$. Both $\mathbf{X}_i$ and $\mathbf{Z}_i$ are made of known constants reflecting the way in which the experimental activity is modelled. They are referred to as fixed-effects and random-effects design matrix, respectively.

The selection among the models A, B, C, D and E with different variance-covariance matrix for the random effects is made in accordance with the Bayesian information criterion (BIC) [19], which is implemented in the function `anova` of the library `nlme` [16]. This function, when given two or more fitted models as parameters computes

the BIC for each of them and performs likelihood ratio tests (LRT) comparing pairs of models in a sequence from the most specific to the most general. The same function `anova`, when given a single model as a parameter, is also used to test the significance of the fixed effects $\boldsymbol{\beta}$. It enables in fact the null hypothesis of equality of all the fixed effects different from β_0 to be tested, namely $H_0: \quad \beta_1 = \beta_2 = \beta_3 = 0$. These β_r's with $r = 1, 2, 3$ constitute the deviations of the expected response (v_0, v_e, t_e, ...) for the $r-th$ material from the expected response for the material associated with β_0. Therefore this allows to conclude from the data whether the electrode materials investigated (Ag, Ni, Ti, W) exert a significant effect on the electrical quantity considered in a specific model fitting procedure.

Model E is a fixed-effects linear model. So its parameters rather than being estimated using the REML method are estimated using the ordinary least square method (OLS) which is implemented in the function `lm` of the `R` environment [18].

Once the parameters of the models have been estimated via REML or OLS, the assumptions underlying the fitted models are also considered by examining the realized residuals. If these realized residuals are inconsistent with the hypotheses of the model (for instance normality and homoschedasticity of the errors), then new models are fitted with similarities to the examples presented in Pinheiro and Bates [16].

The values of the BIC obtained for the five models examined (A, B, C, D and E) are displayed in table 5. In the same table, are also shown the p-values of the test $H_0 : \beta_r = 0 \quad r = 1, 2, 3$, $H_1 : \beta_{\bar{r}} \neq 0$ for at least one $\bar{r} \quad \bar{r} = 1, 2, 3$. For each electrical quantity, the test was conducted on the model with minimum BIC. Due to the fact that the p-values are extremely small, very strong evidence of the effect of the electrode materials on each of the nine electrical quantities considered cannot be denied.

The selection of the model summarised in table 5, is critically examined in the next subsections.

[Table 5 about here.]

5.1. Voltage

The model fitting the measured open circuit voltage (v_0) and having minimum BIC, model E, does not include any effect of the experimental unit. The analysis of the realised residuals does not exhibit major significant departures from the hypotheses underlying the model.

As regards the discharge voltage v_e, the model with minimum BIC is again model E. In figure 5 *(a)* a strip plot of the discharge voltage is shown where the data are grouped by experimental unit (I,II,III,IV,V) ordered by increasing maximum of the voltage inside each group. In each experimental unit the four material investigated (Ag, Ni, Ti and W) are also identified. In this strip plot, the variability of the data does not appear to be different for the different experimental units. The data pertaining to the same material exhibit comparable variability and mean within different experimental units. These considerations suggest that the random factor experimental unit does not exert

any main effect on v_e and that no interaction is present between material and block. The selection of model E quantitatively confirms such graphical observations. The effect of the material on v_e is also visible in this strip plot.

Due to the apparent lack of any effect of the experimental unit on the discharge voltage, all the data regarding the same material in different blocks have been grouped together in the notched box plot of the figure 5 *(b)*. Each box is delimited by the first and the third quartile of the 25 values of v_e in each group and is added with two 'whiskers'. The median of these values appears in this figure as the thicker vertical segment joining the two 'v'-shaped notches in each box. When considering each of the six possible pairs of materials in the figure, if the notches around the two medians do not overlap, then these two medians are significantly different at approximately 95 % level. Detailed description and applications of notched box plots are in McGill *et al* [20].

Discharge voltages measured during μ-EDM operations performed on different pure metal electrodes are significantly different, regardless of the set-up of the generator and the dielectric being identical.

From both strip and box plots of figure 5, it can also be suspected that the variability of the discharge voltage is greater when machining Ti rather than when machining the other metals. This possibility has been investigated by analysing the residuals of model E in two different directions.

First a Levene's test was performed on the residuals grouped by material. Assessing the null hypothesis of equal variability between these grouped residuals resulted in a p-value of 9.4 %. However, Boos and Brownie [21] reported that Levene's test can be conservative, i.e. the computed p-value may overestimate the actual p-value when some deviation from normality is present in the underlying distribution.

Then, a fixed effect linear model with variance of the errors structured in two groups, Ti and the other materials, was fitted to the data. These kinds of models are also known as generalised least squares models (GLS) or extended linear models. The fitting was performed in `R` using the REML method , which is implemented in the function `gls` of the library `nlme` [16]. The variance structure of the residuals was modelled using the variance function `varIdent` of the same library. The BIC of the resulting fitted model is 270.4 and makes it preferable to model E (BIC=272.9). This additional model does not change the conclusions regarding the effect of the electrodes materials on the mean of v_e. However, its small BIC value suggests that the electrode material may have a significant effect also on the variability of the discharge voltage.

[Figure 5 about here.]

5.2. Current

The selection of model C for the measurements of discharge duration t_e (table 5) leads to conclude that the experimental unit is a significant source of variability for t_e. The variability of the discharge duration appears particularly sensitive to the experimental

conditions. Moreover, in each block, the electrode material is an additional source of significant variability for t_e. In model C, the effects of block and material are not correlated and the variability of t_e accounted for by the material is the same for each block. A strip plot of the residuals grouped by material highlighted a strong dependence of their variance on the electrode materials investigated. Like in the case of the discharge voltage, a new model was therefore considered with the errors having different variances for each level of the stratification variable electrodes material S_{ij}, namely:

$$\mathrm{Var}\,(e_{ij}) = \sigma^2 \cdot \delta^2_{S_{ij}} \quad i = 1, \ldots, 5 \quad j = 1, \ldots, 20 \tag{2}$$

In the case examined, it holds $S_{ij} \in \{\mathrm{Ag}, \mathrm{Ni}, \mathrm{Ti}, \mathrm{W}\}$. The fitting was performed in `R` using the functions `varIdent` and `lme`. The BIC of the resulting model is 1084.2, which is better than C's (1088.8), whereas the p-value for the significance of the fixed effect remains substantially as given in table 5. Other examinations of the realised residuals do not show significant violation of the assumptions underlying both model C and its extension.

This analysis of the measurements of t_e leads to the conclusion that the electrodes materials have a significant effect on both mean and spread of the discharge duration. The notched box plot of the discharge duration measurements grouped by material is provided in figure 6 and graphically support such a conclusion.

[Figure 6 about here.]

Regarding the discharge current $\bar{I}$, model B has minimum BIC. However, the subsequent analysis of the realised residuals, of the predicted random effects and of the estimated parameters reveal a number of inconsistencies with the assumptions of the model. In particular the variance of the random effect associated with silver is substantially zero, while the variances of the other random effects are not. Moreover the variance structure of the random effects $\mathbf{b}$ in model B fails to represent fully the effect of the electrode material on the variability of $\bar{I}$. The realised residuals in fact seem to have different spread for different materials (like in the case of t_e).

In figure 7 *(a)* , the discharge current data are grouped by material and, within each material, sub-groups by experimental unit are also identifiable. The vertical lines in each panel are the average $\bar{I}$'s of all the measurements regarding a material. For Ni, Ti and W, the dispersions of $\bar{I}$ appear comparable, whereas for Ag the spread is suspected to be significantly smaller. These observations are also confirmed in the notched box plot of figure 7 *(b)*, by taking notice of the different sizes of the boxes, which are associated with the interquartile range. In this box plot, the groups consists of 25 measurements of $\bar{I}$, which were obtained by pooling together data for the same material across the five blocks. The medians of the discharge current for Ni and Ti appear significantly different from all the others, whereas Ni and Ag have comparable medians at approximately 95 % significance level.

As a results of all the observations above, new models where fitted to the data. Among these, the model with minimum BIC was obtained by introducing a variance structure for the errors in model C. As described by equation 2, each material was

associated to a different errors variance. Moreover, Ni and W were assumed to have the same errors variance. In this manner, a new model with BIC=1078.4 was obtained. Its realised residuals do not present major violations of the underlying assumptions. The p-value for the test $H_0 : \beta_r = 0$ with $r = 1, 2, 3$ is 0.13 %.

On the basis of this analysis, it is then concluded that the electrode material has a significant effect on both mean and variability of the discharge current. Moreover, due to the significance of the block random effect, the dispersion in the measurements of this current appears sensitive to the experimental conditions.

[Figure 7 about here.]

The maximum current I_{max} is significantly affected by the electrode material in both mean value and variability. But it does not exhibit significant sensitivity to the experimental conditions. These are the conclusions drawn by observing that the residuals of model E, which has minimum BIC, display two different spreads. The first characterises Ag, Ni and W, whereas the second, which is larger, Ti. This evidence is confirmed by fitting the data with a GLS model having the errors with two different variances. The first is for the errors associated with Ag, Ni and W, while the second is for those associated with Ti. The corresponding BIC is -216.1 and the p-value for the test $H_0 : \beta_r = 0$ with $r = 1, 2, 3$ is 0.01 %. In figure 8 *(a)*, a notched box plot of the measurements of maximum current grouped by material also supports these conclusions.

As regards t_{max}, model B, which has the minimum BIC, has a null estimate of the variance of the random effect connected with W. This is inconsistent with the assumption of the model itself, which unnecessary dedicates a model parameter to such a variance. Furthermore, the realised residuals of this model show different spreads for different materials in violation of the assumed homoschedasticity of the errors. New models have therefore been fitted. The minimum BIC of 742.8 was achieved for model C, where the errors have been stratified for different materials according to equation 2. Consequently, it is argued that the measurements of t_{max} have significantly different mean and variability when machining different electrode materials. These measurements are also sensitive to the experimetal conditions (in model C the effects of the experimental units are significant). The notched box plot in figure 8 *(b)* provides a graphical confirmation of the effects of the electrode materials.

The ratio I_{max}/t_{max} may give some indication of the time required to break the in-between-the-electrodes dielectric. In this view, it may moreover be thought of as contributed to by the degree of contamination of the inter-electrodes dielectric in an inversionally proportional way. This contamination of the dielectric may be different for different electrode materials. In fact the removal mechanism may be affected by the different physicochemical properties of the electrode materials. For instance, during the removal action, different electrode materials may produce gases and debris with different properties in the inter-electrodes gap. A box plot of the realised ratios groupped by material is shown in figure 8 *(c)*.

A model was fitted to the data I_{max}/t_{max} and a significant effect of the electrode materials on both the mean and the variability of such ratio was found. In fact, the minimum BIC model is without any random effects (model E), but with variance of the errors different for different materials (variances associated with W and Ag comparable, but significantly larger variances for Ni and Ti). The p-value for the test $H_0 : \beta_r = 0$ with $r = 1, 2, 3$ is less than 0.01 %. Further investigation is required to quantify the proportion of this effect associated to presently uncontrollable local micro conditions. For instance, the nature of the local turbulence in the dielectric flow between the electrodes.

[Figure 8 about here.]

5.3. Instant power and energy

The selection of model C (BIC=374.0) indicates that the variability of discharge power measurements $\bar{P}$ is affected by both electrode materials and experimental units. A p-value $< 0.01\,\%$ in the test $H_0 : \beta_r = 0$ with $r = 1, 2, 3$ is a strong indication that the electrode materials significantly affect the mean of the discharge power. An examination of the realised residuals does not show major discrepancies between measurements results and model's assumptions. Graphical summaries of the measurements of $\bar{P}$ are displayed in figure 9 *(a)* and 9 *(b)*.

As regards the maximum power P_{max}, model C, which has the minimum BIC (510.0), gives an estimate of $\sigma_{main} = \sigma_{block}$ which is not significantly different from zero. This makes the number of parameters in model C larger than necessary. An examination of the realised residuals then shows an effect of the electrode materials on the variability of the residuals themselves. These considerations suggest that the experimental data are better interpreted by a model without random effects due to the experimental units.

A number of alternative models with different variance structure of the errors were considered. Model E was selected because of the considerations above and owing to the fact that its BIC (514.3) is closest to the minimum in table 5 (510.0). Its realised residuals do not show any denial of the hypotheses underlying the model. Consequently, no significant effect of the material on the variability of P_{max} is present.

A confidence interval for the standard deviation of the errors, σ, provides an indication of the capability of the process in terms of maximum electrical power. Under the assumptions of the model, a 95 % confidence interval is given by the following expression:

$$\sqrt{\hat{\sigma}^2 \cdot \frac{(n-p)}{\chi^2_{n-p,\,1-\alpha/2}}} \leq \sigma < \sqrt{\hat{\sigma}^2 \cdot \frac{(n-p)}{\chi^2_{n-p,\,\alpha/2}}} \tag{3}$$

where $\hat{\sigma}$ is the estimated standard deviation of the errors (1.55 W), n is the overall number of measurements (100), p is the number of parameters associated with the fixed effects (4), $\alpha = 95\,\%$, $\chi^2_{n-p,\,1-\alpha/2}$ and $\chi^2_{n-p,\,\alpha/2}$ are the quantiles of the chi-squared distribution that has $n - p$ degrees of freedom and with probability $1 - \alpha/2$

and $\alpha/2$ at their left, respectively. The 95 % confidence interval for σ therefore is $2.564\,\mathrm{W} \leq \sigma < 3.408\,\mathrm{W}$. Identical results are obtained by fitting the linear model with the `gls` function and by applying to the resulting object the function `intervals`, where both functions belong to the `nlme` library [16]. Such an interval is then expressed in percentage of the overall average measurements of P_{max} across all the electrode materials (60.421 W), producing the adimensional result $4.244\,\% \leq \sigma < 5.640\,\%$. The test $H_0 : \beta_r = 0$ with $r = 1, 2, 3$ produces a p-value $< 2.2 \cdot 10^{-16}$, which confirms the significant effect of the electrode material on the mean of P_{max}. The strip plot and the notched box plot respectively shown in figure 9 *(c)* and 9 *(d)* seem to agree with the conclusions of the quantitative analysis.

The measurements of the discharge energy are respectively displayed in the strip plot and in the notched box plot of figure 9 *(e)* and 9 *(f)*. The discharge energy is significantly affected by the electrode materials both in mean and variability. This conclusion can be drawn from the figures in table 5, where model C has minimum BIC (288.2). This indicates that the model fitting the data the best (according to the Schwarz's BIC) requires a significant contribution to the variability of the discharge energy from both electrode materials and experimental unit. The significance of the material effect on the mean of the discharge energy is instead inferred by observing that p-value is less than 0.01 % in the test $H_0 : \beta_r = 0$ with $r = 1, 2, 3$ (table 5). No major departures from the hypotheses underlying the model are found in an examination of the realised residuals.

[Figure 9 about here.]

6. Conclusions

Operational definitions of electrical quantities characteristic of the phenomena occurring in the in-between-the-electrodes dielectric during μ-EDM operations have been proposed. They are based on the concept of average waveform also defined in this paper.

Measurements of these quantities have been performed on a number of electrodes made of Nickel, Silver, Tungsten and Titanium with degree of purity greater than 99.95 %. All the tests on each of the metals were carried out with an identical set-up on the same machine.

The acquired experimental evidence showed that all the investigated electrode materials have a significant effect on the means of the defined electrical quantities. This implies that it is not possible to pre-determine generator set-ups independently from the electrode material in order to obtain pre-specified levels of the discharge voltage, duration, current, power and energy. In fact, the performed analysis shows that each material is associated with significantly different discharge voltage, duration, current, power and energy. This evidence contrasts with the practice of including in manuals of EDM machines some specifications of generator set-ups to achieve pre-determined levels of discharge current, voltage, time, power and energy for generic classes of materials

(for instance 'steel', 'copper'). In reality these classes may include a number of different specific materials encompassing a large variety of different physicochemical properties, chemical compositions and metallographic structures.

Electrode materials also significantly affect the variance of all the examined electrical quantities, with the exception of the maximum discharge power. In this case, the standard deviation of the natural variability of the process was estimated to lie within the interval $4.244\,\% \leq \sigma < 5.640\,\%$ with confidence level 95 %. The percentage in the expression of σ is referred to the mean maximum power investigate (60.421 W).

By examining the studies of Dibitonto *et al* [11] and Patel *et al* [12] which present increasing discrepancies between the predictions of their models and their experimental data for decreasing discharge energies, together with the results of Singh and Ghosh [14] and of Valentinčič *et al* [22], it can be argued that the material removal mechanism in μ-EDM is not yet fully understood. However, the material removal from the electrode-workpiece must be somehow logically considered as mainly caused by the investigated discharge power and energy.

Acknowledgments

This work was partially performed within the developments of the project 'Launch-Micro' (funded by the European Commission in the Sixth Framework Program) and of the program 'Cardiff University Innovative Manufacturing Research Centre' (funded by the UK Engineering and Physical Sciences Research Council).

References

[1] T Masuzawa 2000 *Annals of the CIRP* **49/2** 473–488
[2] Egashira K, Matsugasako A, Tsuchiya H and Miyazaki M 2006 *Precision Engineering* **30** 414–420
[3] Sémon G 1975 *A Practical Guide to Electro-Discharge Machining - Second Edition* Ateliers des Charmilles S. A. Geneva
[4] Han F, Wachi S and Kunieda M 2004 *Precision Engineering* **28** 378–385
[5] Dauw D 1986 *Annals of the CIRP* **35/1** 111–116
[6] Weck M 1991 *Annals of the CIRP* **41/1** 243–246
[7] Cogun C 1990 *International Journal of Machine Tools and Manufacture* **30** 19–31
[8] Ivanov A, Ferri C, Petrelli A and Popov K 2007 *IPROMS 2007 - Proceedings of the Third International Virtual Conference on Innovative Production Machines and Systems* pp 337–344 ISBN 978-1904445-52-4
[9] Zahn M 1999 *Wiley Enciclopedia of Electrical and Electronics Engineering - Volume 4* ed Webster J G (Wiley) pp 89–123
[10] Beroual A, Zahn M, Badent A, Kist K, Schwabe A J, Yamashita H, Yamazawa K, Danikas M, Chadband W G and Torshin Y 1998 *IEEE Electrical Insulation Magazine* **14** 6–17
[11] Dibitonto D D, Eubank P T, Patel M R and Barrufet M A 1989 *Journal of Applied Physics* **66** 4095–4103
[12] Patel M R, Barrufet M, Eubank P T and Dibitonto D D 1989 *Journal of Applied Physics* **66** 4104–4111
[13] Eubank P T, Patel M R, Barrufet M and Bozkurt B 1993 *Journal of Applied Physics* **73**
[14] Singh A and Ghosh A 1999 *International Journal of Machine Tools & Manufacture* **39** 669–682

[15] Ferri C, Petrelli A and Ivanov A 2007 *IPROMS2007 - Third Virtual International Conference on Intelligent Production Machines and Systems* pp 329–336 ISBN 978-1904445-52-4
[16] Pinheiro J C and Bates D M 2000 *Mixed-Effects Models in S and S-Plus* (Springer) ISBN 0-387-98957-0
[17] Han F, Yamada Y, Kawakami T and Kunieda M 2006 *Precision Engineering* **30** 123–131
[18] R Development Core Team 2006 *R: A Language and Environment for Statistical Computing* R Foundation for Statistical Computing Vienna, Austria ISBN 3-900051-07-0 URL `http://www.R-project.org`
[19] Schwarz G 1978 *The Annals of Statistics* **2** 461–464
[20] McGill R, Tukey J W and Larsen W A 1978 *The American Statistician* **32** 12–16
[21] Boos D D and Brownie C 2004 *Statistical Science* **19** 571–578
[22] Valentinčič J, Duhovnik L, Kušer D and Junkar M 2007 *Proceedings of the* 9^{th} *International Conference on Management of Innovative Technologies - MIT2007* ed Junkar M and Levy P pp 225–228 ISBN 978-961-6536-19-6

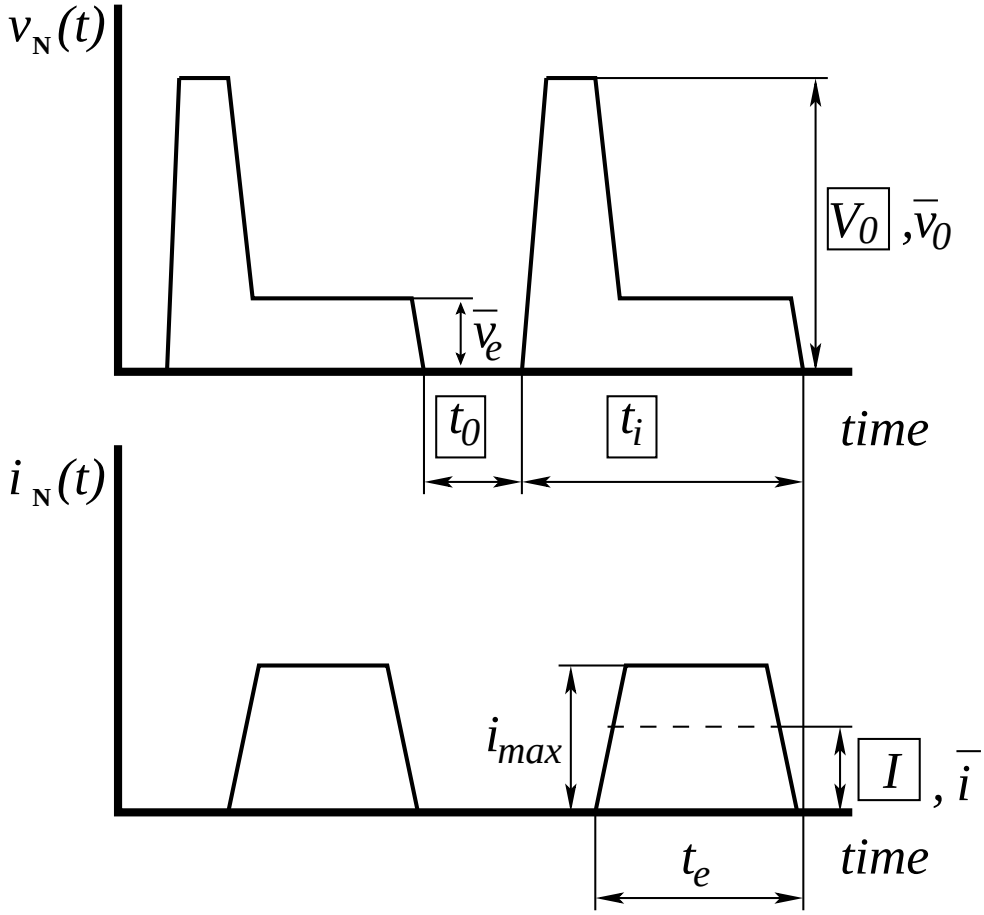

Figure 1. Nominal pulse shapes: typical set-up parameters of a power generator are in boxes, whereas measured parameters are not.

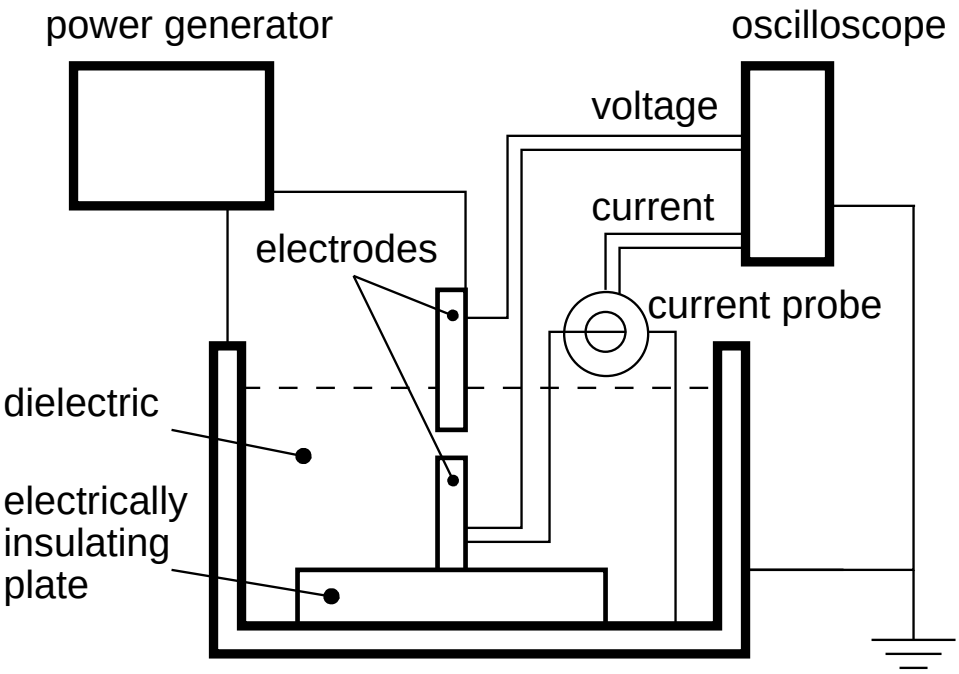

Figure 2. Schema of the test rig.

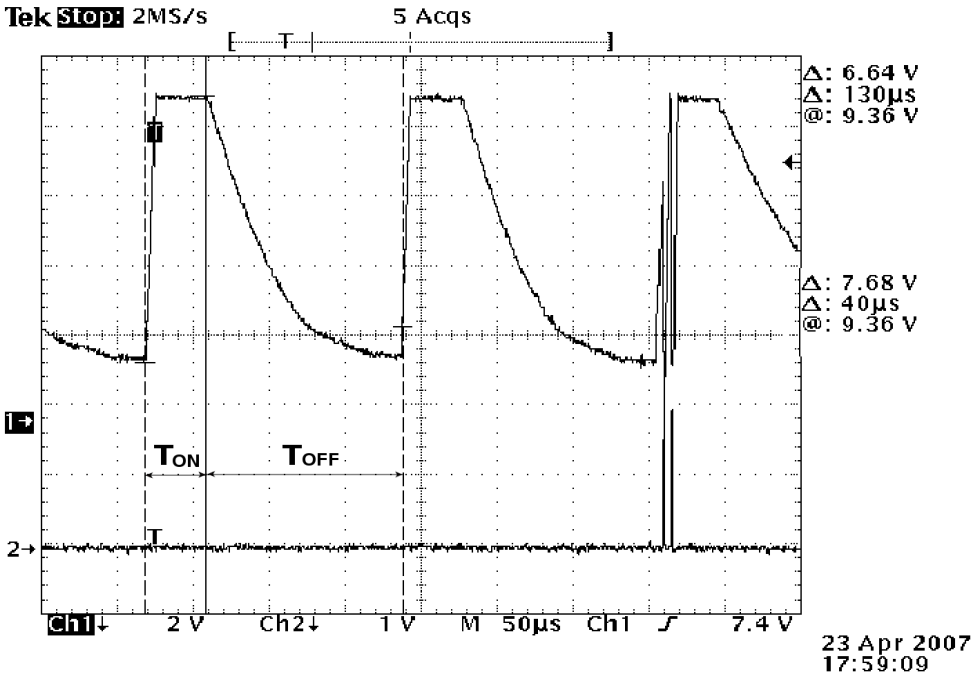

Figure 3. Interpretation of T_{ON} and T_{OFF}.

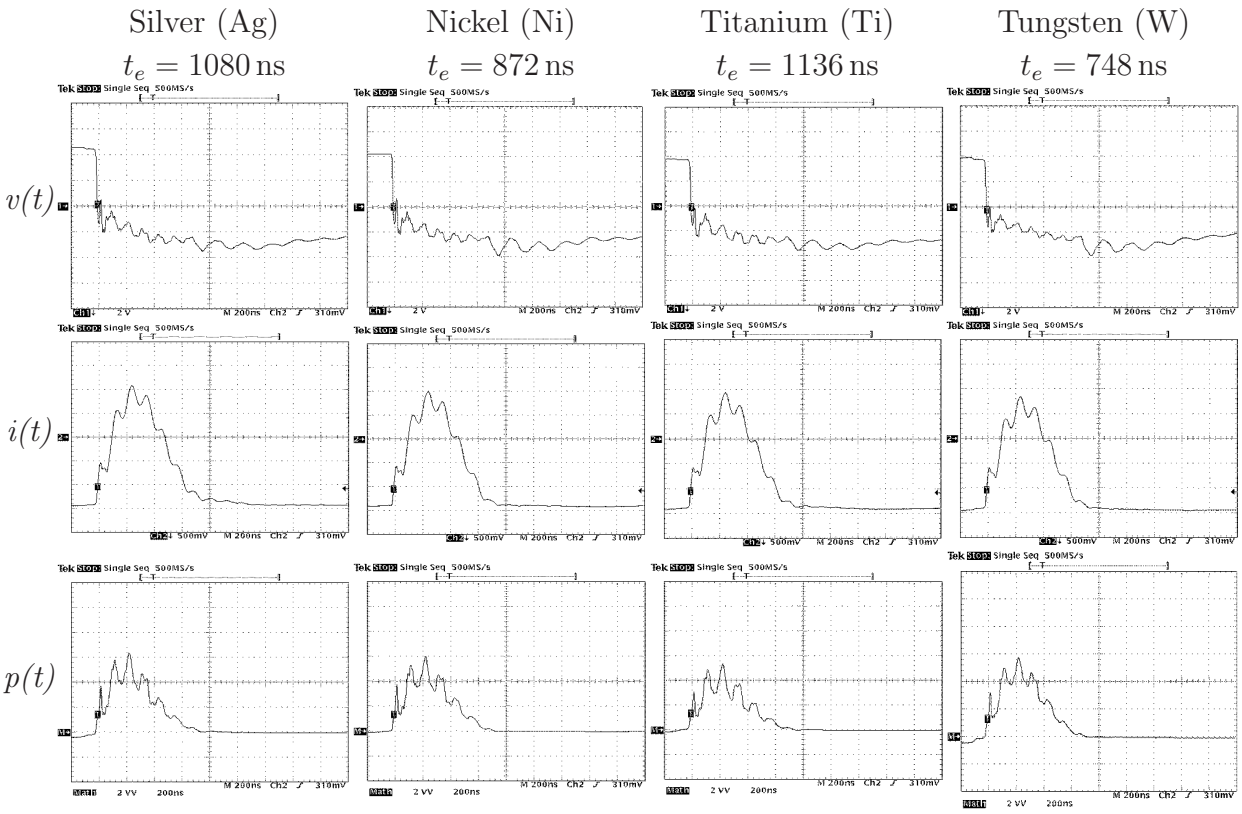

Figure 4. Four cases of voltage, current and instant power generic discharges, designated with *v(t)*, *i(t)* and *p(t)* respectively. They refer to the four electrodes metals investigated (Ag, Ni, Ti, W).

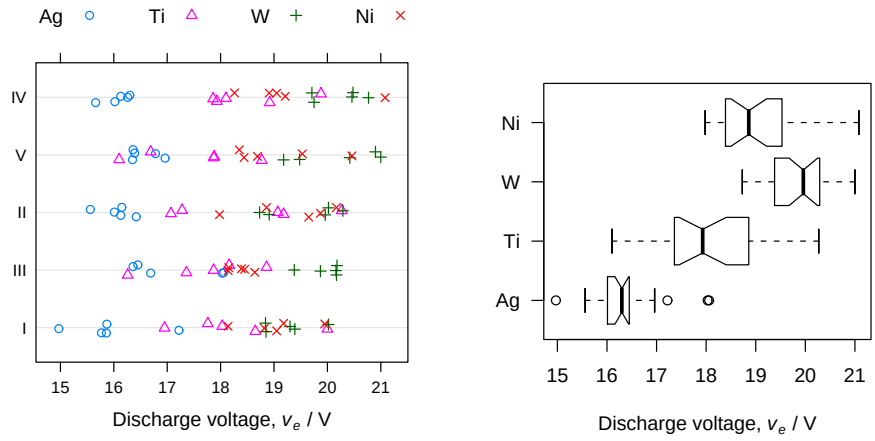

(a) *(b)*

Figure 5. Strip plot *(a)* and notched box plot *(b)* of v_e grouped by experimental unit (20 data per unit) and materials (25 data per group), respectively.

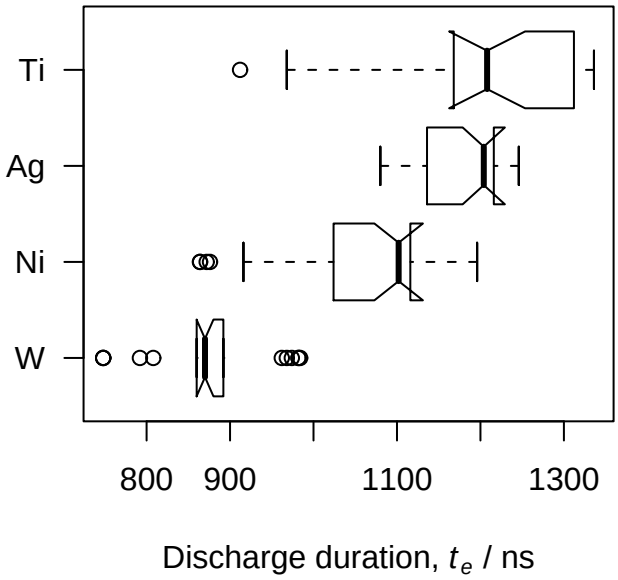

Figure 6. Notched box plot of the measurements of discharge duration grouped by electrodes materials (25 measurements in each group).

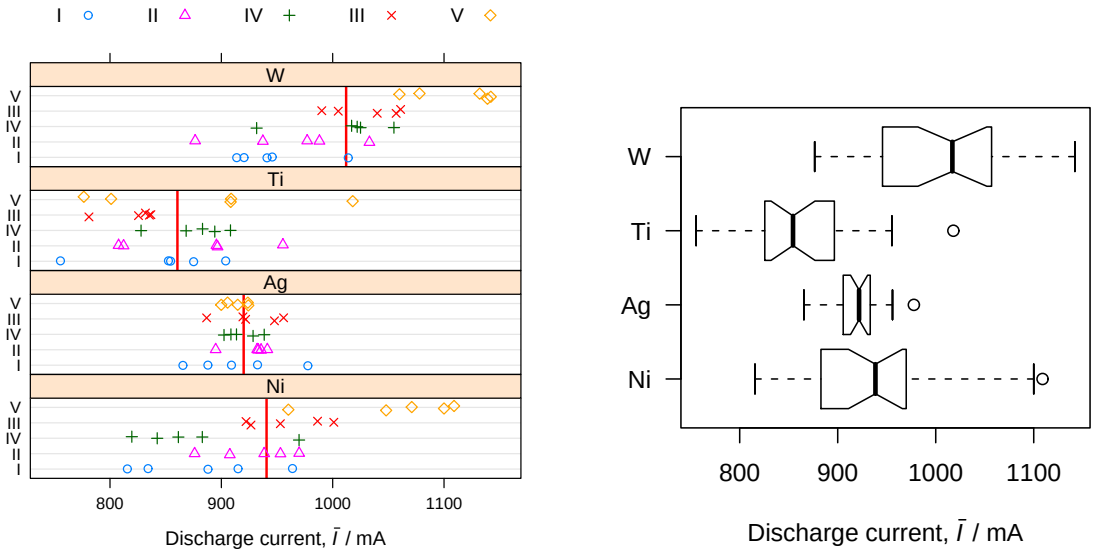

(a) *(b)*

Figure 7. Strip plot *(a)* and notched box plot *(b)* of $\bar{I}$ measurements grouped by materials (25 data per group).

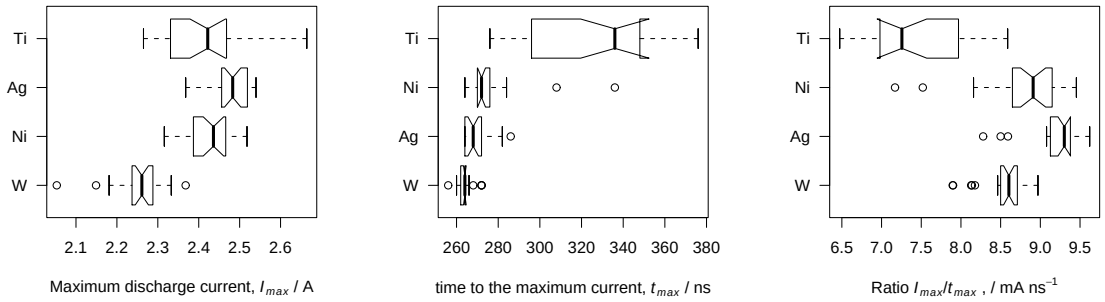

(a) *(b)* *(c)*

Figure 8. Notched box plots of: *(a)* the maximum current, I_{max}; *(b)* the time to the maximum current, t_{max}; *(c)* the ratio I_{max}/t_{max}. All measurements are grouped by electrode materials (25 data per group).

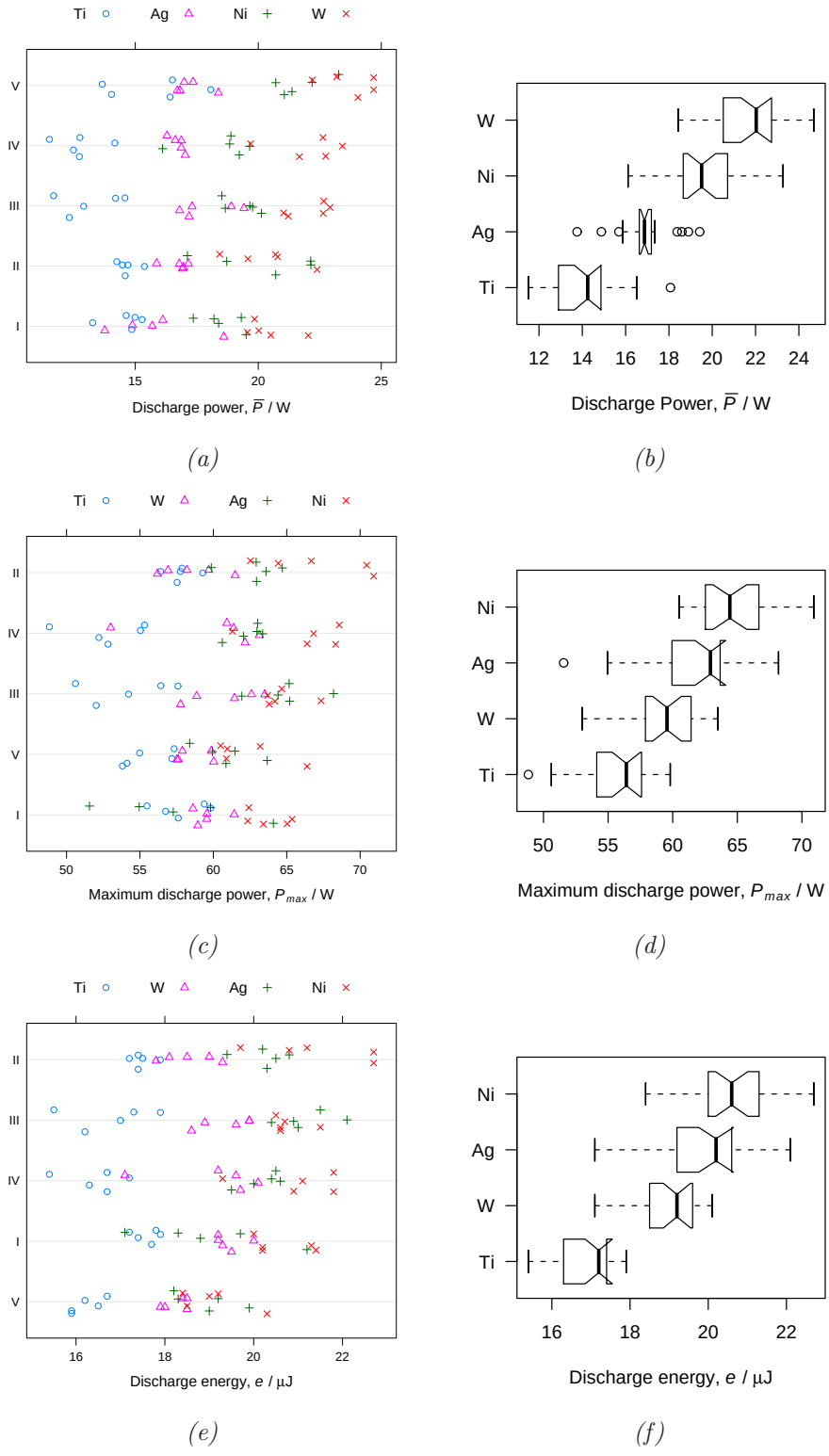

Figure 9. Strip plots *(a)*, *(c)*, *(e)* and notched box plots *(b)*, *(d)*, *(f)* of discharge power, maximum discharge power and discharge energy grouped by experimental unit (20 data per unit) and materials (25 data per group), respectively.

Table 1. Set-up parameters of the EDM generator.

Parameter	Symbol/Unit	Value
Open circuit voltage	V_0/V	80
Mean nominal current	I/A	0.5
Time-on	T_{ON}/μs	1
Time-off	T_{OFF}/μs	1
Reference voltage of the servo system[a]	V_{SERVO}/V	50

[a] Regarding the way this value is internally used in the equipment, no further information is available in the documentation provided by the manufacturer.

Table 2. Technical specifications of the current transformer.

Parameter/Unit	Value
Nominal sensitivity/V A^{-1}	1
Nominal rise time/μs	7
Nominal DC saturation current/A	3
Nominal Maximum rms current/A	7
Nominal low frequency cut-off of the $3\,dB$ bandwidth (sinewave)/Hz	130
Nominal high frequency cut-off of the $3\,dB$ bandwidth (sinewave)/MHz	60
[a]Actual low frequency cut-off of the $3\,dB$ bandwidth (sinewave)/Hz	98
[a]Actual high frequency cut-off of the $3\,dB$ bandwidth (sinewave)/MHz	100
[b]Nominal Maximum Phase shift between signal and current/$^\circ$	≤ 6

[a] The actual bandwidth is the result of a test performed by the manufacturer at the authors' request.

[b] For frequencies in the range of one decade of the cut-off points.

Table 3. Main characteristics of the oscilloscope.

Parameter/Unit	Value
Bandwidth/MHz	200
[a]Vertical resolution/bit	8
[b]Input resistive impedance/MΩ	1
[b]Input capacitive impedance/pF	20 ± 2

[a]This resolution is associated with 25 digitalisation levels per division.
[b] The resistive and the capacitive impedances are in parallel.

Table 4. Main physicochemical properties of the dielectric.

Parameter	Symbol/Unit	Value
Density at 15 °C	ρ/g cm^{-3}	0.765
Kinematic viscosity at 20 °C	ν/cSt	1.8
Flash point °C (Pensky-Martens close cup)	fp/°C	63
Mass fraction of aromatic content	ac/ppm	30
Disruptive voltage at 2.5 mm	dv/kV	58

Table 5. Model selection and highly significant effect of the electrodes materials

		v_0	v_e	t_e	$\bar{I}$	I_{max}	t_{max}	$\bar{P}$	P_{max}	e
	A	442.0	310.4	1111.9	1104.0	-179.6	859.8	402.5	539.1	318.8
	B	417.0	289.0	1107.2	*1082.1*	-204.3	*835.5*	384.7	515.5	298.1
BIC	C	416.6	280.3	*1088.8*	1082.8	-207.6	837.9	*374.0*	*510.0*	*288.2*
	D	414.8	277.5	1097.0	1092.6	-203.9	841.1	378.2	517.4	292.2
	E	*411.6*	*272.9*	1165.6	1103.8	*-207.8*	844.9	392.4	514.3	305.1
$\beta_r = 0$ $r = 1, 2, 3$ *(p-value)*		$< 10^{-15}$	$< 10^{-15}$	$< 10^{-4}$	$< 10^{-4}$	$< 10^{-15}$	$< 10^{-4}$	$< 10^{-4}$	$< 10^{-4}$	$< 10^{-4}$